

Probing the States of Matter in QCD*

Helmut Satz

Fakultät für Physik, Universität Bielefeld
D-33501 Bielefeld, Germany

Abstract:

The ultimate aim of high energy heavy ion collisions is to study quark deconfinement and the quark-gluon plasma predicted by quantum chromodynamics. This requires the identification of observables calculable in QCD and measurable in heavy ion collisions. I concentrate on three such phenomena, related to specific features of strongly interacting matter. The observed pattern of hadrosynthesis corresponds to that of an ideal resonance gas in equilibrium at the pseudo-critical temperature determined in QCD. The critical behavior of QCD is encoded in the fluctuation patterns of conserved quantum numbers, which are presently being measured. The temperature of the quark-gluon plasma can be determined by the dissociation patterns of the different quarkonium states, now under study at the LHC for both charmonia and bottomonia.

1 Feynman's Broken Watch

The high energy heavy ion program was initiated in the nineteen-eighties at CERN and at Brookhaven, and it had a well-defined aim: to produce and study in the laboratory the deconfined state of matter, the quark-gluon plasma, predicted some years earlier by quantum chromodynamics. The charge was thus to create a new state of matter through high energy collisions of heavy nuclei.

The investigation of such collisions is a very multi-faceted enterprise. It involves initial state aspects, parton structure and its limit as color glass, multiple parton interactions, non-equilibrium evolution, thermalization questions, hydrodynamic expansion, viscosity and flow, and much more. The final creation of deconfined thermal systems through such interactions remains a rather speculative issue, and the view of sceptics was perhaps best summarized by Richard Feynman when he said: "if I throw my watch against the wall, I get a broken watch, not a new state of matter". The problem has two inherent aspects. On the one hand, we have to show that the collision leads to a medium with large scale collective behavior, something one would call matter; on the other hand, we want the initial state of this thermal system to be the QCD plasma of quarks and gluons.

* Survey talk given at the 26th *International Symposium on Lepton Photon Interactions at High Energies*, San Francisco, California, USA, June 24 - 29, 2013.

The mentioned non-equilibrium issues are difficult, if not impossible, to account for in terms of first principle QCD calculations. Experimentally, the observation of hydrodynamic flow, both radial and elliptic, shows the presence of collective effects. Moreover, the resulting medium is extremely dense, leading to a strong quenching of high transverse momentum jets. Much interesting theoretical work has been carried out on the interpretation of these results, and this has led to something one might call a split of paradigms. On one hand, one can attempt to model the dynamical collision process in its various stages from partonic beginning to hadronic end and then check to see if the data agree with the model. As interesting as such an approach is, it does not really assure us that the produced medium is indeed the quark-gluon plasma described in non-perturbative QCD studies. To conclude that, there seems to be only one way: to calculate in equilibrium statistical QCD some observable features and then test if these features indeed arise in high energy nuclear collisions. This approach, if successful, will tell us whether we have fully carried out the charge assigned to us at the start of the heavy ion program. The aim of my survey will be this line of study, to identify *ab initio* results from statistical QCD which can be compared to data from high energy heavy ion collisions. Where are we at present in this specific task?

I will in particular cover three issues: are there experimental indications for thermal equilibrium of the produced hadronic medium, and if so, how can we look in heavy ion collisions for the critical features of QCD at the quark-hadron transition? Finally, on the deconfined side, how can we measure in a collision environment the temperature of the produced deconfined environment, the expected hot quark-gluon plasma? The first two of these topics are presently being addressed in fluctuation studies at the CERN-LHC, in a dedicated experiment at the CERN-SPS, and by the beam energy scan at RHIC. The last is a central theme for the heavy ion program of three LHC and two RHIC experiments. With a consideration of these topics, my heavy ion theory report will moreover be quite complementary to those given at the last two Lepton-Photon conferences [1, 2], which have concentrated more on the dynamical evolution aspects of the produced medium.

2 Hadrosynthesis and Freeze-Out

For two massless quark flavors, strongly interacting matter as function of temperature T and baryochemical potential μ shows a two-phase structure, defined by chiral symmetry. At low T and μ , the expectation value of the chiral condensate, $\chi(T, \mu) = \langle \bar{\psi}\psi \rangle$, is non-zero, the chiral symmetry of the QCD Lagrangian is spontaneously broken; with increasing T and/or μ we reach a critical line in the $T - \mu$ plane at which chiral symmetry is restored. The resulting generic phase diagram is shown in Fig. 1(a). More specifically, the transition at $\mu = 0$ is conjectured to be of second order and in the universality class of the three-dimensional O(4) spin system [3]; lattice studies support this and moreover have the second order behavior continue up to some (small) values of μ [4]. At low temperatures, various arguments suggest that the transition is of first order [5]. We thus expect a tricritical point P at the position in the $T - \mu$ plane where the two transition lines meet [6, 7]. The corresponding phase diagram is shown in Fig. 1(b). At small μ , the transition line not only defines chiral symmetry breaking and restoration, but it also separates the state of deconfined quarks and gluons from an interacting hadronic medium.

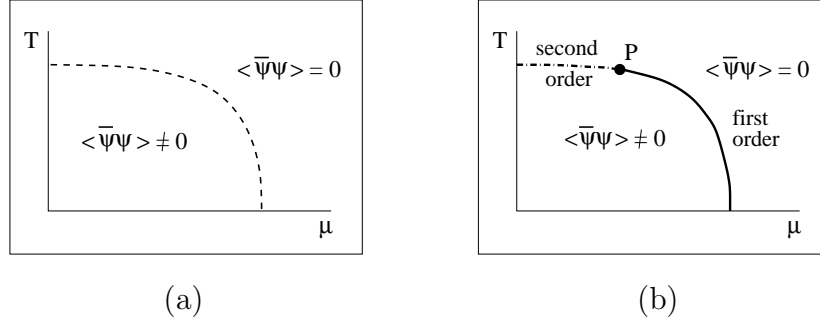


Figure 1: (a) Generic phase diagram for QCD of two massless quark flavors; (b) specific transition structure: second order (dashed line), tricritical point (P), first order (solid line).

The real world has u and d quarks of small but finite masses m_q , and the presence of these masses affects continuous critical behavior in much the same way as an external field does to a spin system - it turns singular behavior into a pseudo-critical rapidly varying cross-over of the relevant physical variables. On the other hand, a first order transition can be modified parametrically, but not removed completely, so that such a transition remains present also for small but finite quark masses m_q . As a result we obtain the pattern shown in Fig. 2(a); the endpoint E of the first order line is now simply critical, with the Z_2 exponents of the three-dimensional Ising model, at which the pseudo-critical cross-over starts.

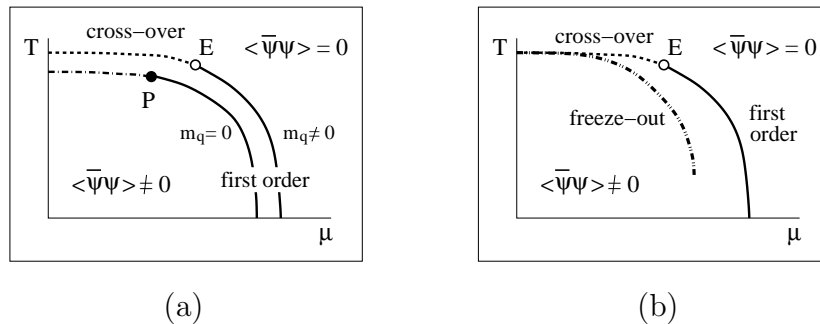


Figure 2: (a) Phase diagram for QCD with $m_q \neq 0$ compared to the case $m_q = 0$; (b) expected freeze-out line compared to the transition line for $m_q \neq 0$.

Adding a third heavier s quark does not significantly change the pattern, so the behavior shown in Fig. 2(a) holds for this case as well. For a system with 2+1 physical quark mass values, the temperature of the transition at $\mu = 0$ is in the latest lattice studies [8] established by calculating the continuum limit of the chiral susceptibility, i.e., the derivative of the chiral condensate with respect to the light quark mass for $m_q \rightarrow 0$. It is found to peak at $T_H = 154 \pm 9$ MeV, see Fig. 3.

If the interactions in the hadronic system appearing just below the transition are resonance-dominated, the newly formed confined medium can be represented as an ideal gas of all possible resonance states [9,10] at one common “freeze-out” temperature T_f . The relative abundances of the different hadron species are then determined at this point; subsequent cooling can change the abundances only through decay, not through interaction. In the

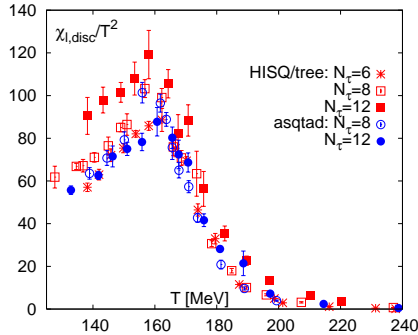


Figure 3: Temperature variation of the chiral susceptibility in (2+1) QCD with physical quark masses [8].

low baryon density limit, i.e., at small or vanishing μ , resonance dominance is a good assumption; we recall the success of the dual resonance model. With increasing μ , however, baryon-baryon interactions begin to play a role, and these are not of resonance nature; hence the freeze-out curve is expected to fall eventually below the chiral transition curve, as shown in Fig. 2(b).

In an ideal gas of hadronic resonances at fixed freeze-out temperature T_f , the abundances of the various species are specified by the corresponding phase space weights. The relative abundance of states i and j is thus given by

$$\frac{N_i}{N_j} = \left(\frac{d_i}{d_j}\right) \left(\frac{m_i}{m_j}\right)^2 \frac{K_2(m_i/T_f)}{K_2(m_j/T_f)} \simeq \left(\frac{d_i}{d_j}\right) \left(\frac{m_i}{m_j}\right)^{3/2} \exp\{-(m_i - m_j)/T_f\}, \quad (1)$$

where m_i denotes the mass and d_i specifies the intrinsic degeneracy (charge, spin) of the state. We have here assumed non-strange mesons; baryon number and strangeness lead to additional factors, to which we shall return shortly. The striking feature observed in high energy heavy ion collisions is that the relative abundances of all observed hadrons, more than a dozen species, are well-described in terms of such a resonance gas, with one common freeze-out temperature $T_f = 160 \pm 10$ MeV [11–16]. In Fig. 4 we give an illustration of the agreement. The slight temperature differences between the two plots arise from an introduction of non-resonant baryon interactions in a more recent version of the model [17]. The distribution of the pieces of the broken watch is thus given by an ideal gas of fixed temperature: the collision does produce something like hadronic matter, and the hadrosynthesis occurs at just the transition temperature predicted by QCD.

There is an interesting caveat to be added here. The abundances of the hadron species produced in elementary interactions (pp , $p\bar{p}$, e^+e^-) are also reproduced with the same or better precision by a thermal resonance gas of the same temperature of 160 MeV, although here one presumably does not create a genuine thermal medium. In these interactions, however, there is one clear deviation from the predictions of an ideal resonance gas model: the abundances of strange particles are systematically lower than the predictions. This has been accounted for phenomenologically by the introduction of a strangeness suppression factor $\gamma_s \simeq 0.5 - 0.6$ [18]; the production rate of a hadrons containing n strange quarks are then reduced by a factor γ_s^n . This one additional parameter then allows an excellent account of all elementary hadroproduction. The origin of this thermal behavior

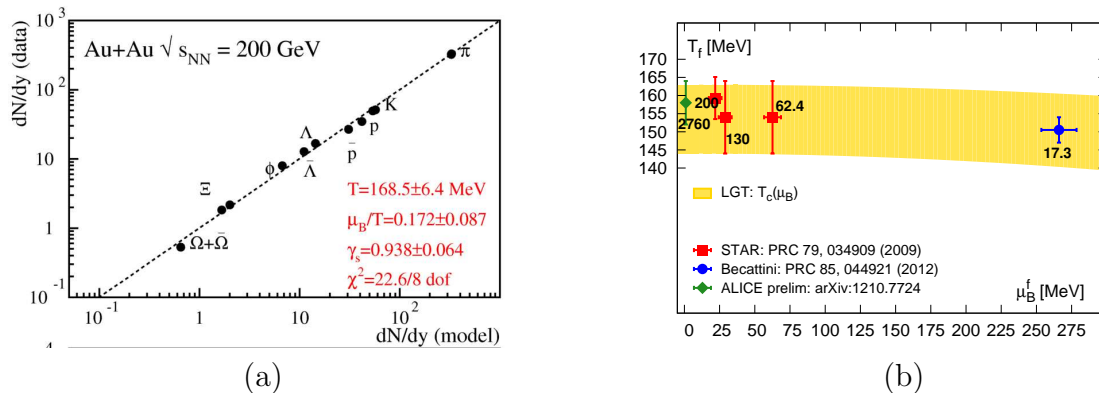


Figure 4: (a) Species abundances in Au-Au collisions; (b) freeze-out parameters in heavy ion collisions at different energies vs. lattice QCD results.

has been an enigma for many years; it is most likely resolved by local stochastic production, initiated by quark tunnelling through the confinement event horizon [19]. Such a scheme in fact provides automatically the strangeness suppression observed for elementary interactions [20].

The mere observation of thermal hadron abundances thus does not establish that a truly thermal medium was formed. A first indication that this is in fact the case in heavy ion collisions is indicated by the convergence of the suppression factor $\gamma_s \rightarrow 1$, which arises from a statistical averaging over the production processes due to the different nucleon-nucleon collisions in the interaction [21]. All abundances, including those of strange hadrons, are now indeed given by an ideal resonance gas.

To further corroborate this claim, one has studied the temperature dependence of conserved quantum numbers in an ideal hadron gas and compared this to both lattice results and heavy ion data. We consider as an illustration the baryon number behavior. The pressure of the hadron gas is then given by the sum over all resonance species up to some mass of around 2.5 GeV (a further increase does not lead to significant changes),

$$\frac{P(T, \mu)}{T^4} = \frac{1}{\pi^2} \sum_i d_i (m_i/T)^2 K_2(m_i/T) \cosh(B_i \mu/T), \quad (2)$$

where B_i denotes the baryon number of the species and μ the corresponding baryochemical potential. The meson contribution, with $B_i = 0$, depends on T only; in general, however, a fit of the observed species abundances thus specifies the two freeze-out parameters T_f and μ_f . For collision energies $\sqrt{s} \geq 20$ GeV, the temperature is found to have the mentioned value of some 160 - 165 MeV; the baryochemical freeze-out value μ_f decreases from about 220 MeV at top SPS energy (20 GeV) to 25 MeV at top RHIC energy (200 GeV) and essentially zero at the LHC. As expected, a variation of the collision energy thus results in a considerable variation of the baryochemical potential; increasing the collision energy leads to more and more nuclear transparency and thus to lower baryon density. This effect can be used to study fluctuations in baryon number. The generalized n -th order baryon number cumulant,

$$\chi_B^{(n)}(T, \mu) = \frac{\partial^n (P/T^4)}{\partial (\mu/T)^n}, \quad (3)$$

is readily calculated from eq. 2, and keeping in mind that only baryons with $B = 1$ enter, one finds relations of the form

$$\frac{\chi_B^{(3)}}{\chi_B^{(1)}} = \frac{\chi_B^{(4)}}{\chi_B^{(2)}} = \frac{\chi_B^{(5)}}{\chi_B^{(3)}} = \dots = 1 \quad (4)$$

for ratios two units apart. For those separated by one unit, one has

$$\frac{\chi_B^{(2)}}{\chi_B^{(1)}} = \coth(\mu/T), \quad \frac{\chi_B^{(3)}}{\chi_B^{(2)}} = \tanh(\mu/T), \quad \frac{\chi_B^{(4)}}{\chi_B^{(3)}} = \coth(\mu/T), \quad (5)$$

and so on. If the confinement transition has led to a hadronic resonance gas in equilibrium, all memories of previous stages are lost, and so an agreement with relations (4)/(5) would indeed confirm the production of *hadronic matter* of a freeze-out temperature $T_f = T_H$ equal to the transition value.

Lattice studies have so far shown that such an ideal resonance gas behavior is also what QCD predicts. As an illustration, we show in Fig. 5(a) results for the second baryon number cumulant χ_2^B in (2+1) flavor QCD, compared to the corresponding hadron resonance gas prediction. Up to the transition temperature, the agreement is excellent. Experimentally, the cumulants can be measured in terms of higher moments of the baryon number dispersion, $N_B - \langle N_B \rangle$, and such data has been obtained by the STAR collaboration at RHIC [23]. Species abundances determine T_f and $\mu(T_f)$ at collision energies of 19.6, 62.4 and 200 GeV. The baryon number fluctuations allow a determination of the cumulant ratios, and the results for three ratios are compared in Fig. 5(b) to the resonance gas predictions (4) and (5) [23]. The agreement is also seen to be quite good.

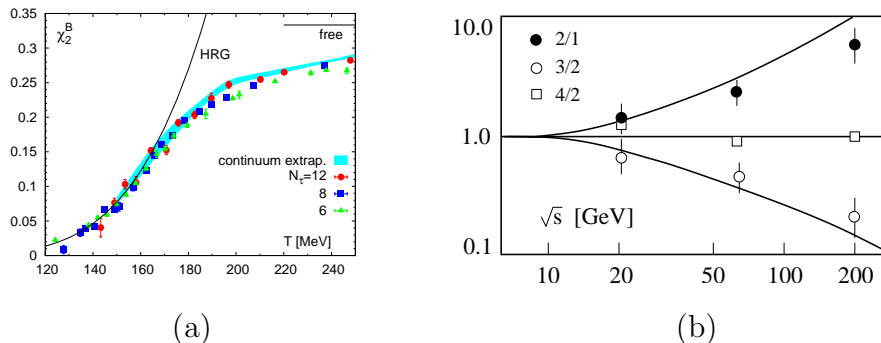


Figure 5: (a) Theory: lattice results (2+1 quark flavors, $\mu = 0$) for the second order baryon number cumulant, compared to the hadron resonance gas form. (b) Experiment: STAR data [22] on baryon cumulant ratios, eqns. (4) and (5), as function of collision energy \sqrt{s} , vs. hadron resonance gas predictions [23] (solid lines).

We thus find that high energy heavy ion collisions produce a medium which can be considered as hadronic matter in equilibrium, formed at the pseudo-critical hadronization temperature predicted by lattice QCD. And cumulant studies show that also correlations in this medium appear to follow the pattern of an ideal resonance gas, which for the lower orders is again in accord with QCD. But evidently we would like more: we want to find in the collision data some sign of the actual transition, of something like critical

behavior. Sufficiently close to a continuous transition, correlations appear at all scales, the correlation length diverges, and in QCD this must produce strong deviations from the ideal hadron gas behavior just studied. What is “close enough”, and what observables should one look at?

3 Critical Behavior: Fluctuations and Correlations

Along the line of the second-order transition and at the tricritical point, thermodynamic observables exhibit continuous critical behavior; this implies in particular that higher order derivatives of the thermodynamic potential diverge in a well-defined functional form specified in terms of the critical exponents of the relevant symmetry group. These derivatives, in turn, express calculable fluctuations of physical observables. For the idealized case considered here, the chiral limit of QCD, we thus obtain predictions for the fluctuations of baryon number, charge and strangeness.

There are two regions of critical behavior of particular interest for heavy ion studies. If the pseudocritical cross-over line for physical values of m_q and small μ is sufficiently close to that of the second order transition in the chiral limit, we may there expect remnants of $O(4)$ criticality, and we can look for them at top RHIC energy and at the LHC. At larger μ and finite m_q , we expect to encounter critical behavior near the end point E of the first order regime, and the main aim of present beam energy scans at RHIC as well as that of the NA61 experiment at the CERN-SPS is the search for this end point through its effect on the freeze-out line. Here the exponents are those of the Z_2 group. In both cases, near $\mu = 0$ and near the critical endpoint at finite μ , we are thus looking for *remnants of criticality* (see Fig. 6). The pseudo-critical line near $\mu = 0$ approaches the critical line only in the chiral limit $m_q \rightarrow 0$, and the freeze-out line at finite μ is off the line of first order transition and the critical endpoint by the presence of non-resonant interactions.

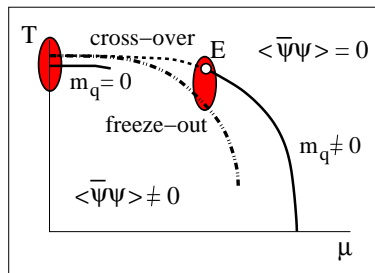


Figure 6: Phase space regions proposed to look for remnant critical behavior.

What can we calculate and what can we look for? Since the overall critical structure of QCD as function of T , μ and m_q is somewhat involved, let us first look at a simpler case for illustration, the Ising model of spins $s_i = \pm 1$ on a three-dimensional spatial lattice of N^3 sites. It is defined by the Hamiltonian

$$\mathcal{H} = -J \sum_{\{i,j\}} s_i s_j - H \sum_i s_i, \quad (6)$$

where J specifies the interaction of next-neighbor spins and H a possible external field. For $H = 0$, the system is Z_2 symmetric; the Hamiltonian then remains invariant under

spin flip $s_i \rightarrow -s_i \forall i$. The thermodynamics is encoded in the partition function

$$Z(T, H) = \prod_{i=1}^{N^3} \sum_{s_i=\pm 1} \exp \{-\beta \mathcal{H}\}, \quad (7)$$

where $\beta = 1/T$ is the inverse temperature; this in turn leads to the density of the (Helmholtz) free energy

$$f(T, H) = -\frac{T}{V} \log Z(T, H), \quad (8)$$

with $V = N^3$. At first sight, it seems to vary smoothly with T and H ; to show explicitly the critical behavior inherent in the system, we have to look at derivatives with respect to T and H , at the so-called *response functions*. The first temperature derivative specifies the energy density

$$\epsilon(T, H = 0) \sim \left(\frac{\partial f(T, H)}{\partial T} \right)_{H=0} \quad (9)$$

and still shows continuous behavior, but the second, the specific heat,

$$c_v(T, H = 0) \sim \left(\frac{\partial \epsilon(T, H)}{\partial T} \right)_{H=0} \sim \left(\frac{\partial^2 f(T, H)}{\partial T^2} \right)_{H=0} \sim |T - T_c|^{-\alpha} \sim |t|^{-\alpha}, \quad (10)$$

diverges as a power at a critical temperature T_c ; hence we use from now on $t = (T - T_c)/T_c$ as suitable variable, with the critical exponent α specifying the singular behavior. In Fig. 7, we illustrate the resulting patterns schematically. Included are here also the next two derivative orders, and in all cases, we also show the expected pattern if the symmetry is slightly broken by the presence of a small external field H . We note in particular the non-monotonic behavior of all derivatives higher than the energy density; this behavior signals criticality and clearly deviates from any resonance gas pattern.

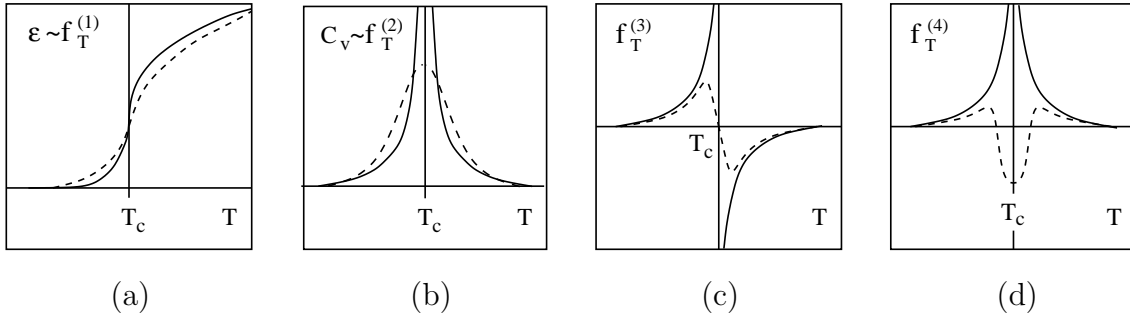


Figure 7: 3d Ising model response functions up to fourth order, for $H = 0$, solid line, and for small finite external field H , dashed line.

The other variable H leads to a similar pattern. The first derivative with respect to H gives at $H = 0$ the spontaneous magnetisation,

$$m(t, H = 0) \sim \left(\frac{\partial f(T, H)}{\partial H} \right)_{H=0} \sim |t|^\beta, \quad (11)$$

for $t < 0$; for $t \geq 0$, $m(t, H = 0) = 0$: the magnetisation is the order parameter and thus vanishes above the critical point for $H = 0$. For finite H , it remains finite even there,

vanishing as

$$m(t=0, H) \sim \left(\frac{\partial f(T, H)}{\partial H} \right)_{t=0} \sim h^{1/\delta}, \quad (12)$$

along the critical isotherm, with $h = H/T_c$. The second derivative

$$\chi_T(t, h=0) \sim \left(\frac{\partial m(t, h)}{\partial h} \right)_{h=0} \sim \left(\frac{\partial^2 f(t, h)}{\partial h^2} \right)_{h=0} \sim |t|^{-\gamma}, \quad (13)$$

gives the isothermal susceptibility, the rate at which the magnetisation vanishes at the Curie point; it also diverges there. In summary: critical behavior means that higher order derivatives of the pressure diverge in a functional form specified by critical exponents (we here had α , β , γ and δ) which are fixed once the symmetry group is given.

The singular behavior of the response functions can in turn be related to that of fluctuations and correlations. The specific heat determines the energy fluctuation over the lattice,

$$c_V(T) \sim \langle (\sum_{i,j} s_i s_j)^2 \rangle - \langle \sum_{i,j} s_i s_j \rangle^2 \quad (14)$$

while the susceptibility measures the fluctuation of the spin,

$$\chi_T(t, H=0) \sim \langle (\sum s_i)^2 \rangle - \langle \sum s_i \rangle^2; \quad (15)$$

in the absence of spin-spin correlations, it vanishes. The divergence of the response functions at the critical point is thus connected to fluctuations diverging there, which in turn is a consequence of diverging correlations: at the critical point, the spin-spin correlation length ξ diverges as

$$\xi(t) \sim |t|^{-\nu}, \quad (16)$$

so that constituents of all scales become correlated (critical opalescence). Given sets of lattice configurations at various temperatures, we can thus, through the calculation of response functions, determine the onset and the analytical form of the critical behavior shown by the system. Using the form (16), one can also express the response functions in terms of the correlation length. For the 3d Ising model, the specific heat becomes

$$\chi_T \sim \xi^{\gamma/\nu} \sim \xi^2, \quad (17)$$

using $\gamma \simeq 1.2$, $\nu \simeq 0.6$ for the 3d Ising model; higher derivatives grow as higher powers of ξ .

In the case of QCD, we have in addition to the temperature the chemical potentials of the conserved quantum numbers as thermodynamic parameters, μ_B for the baryon number, μ_Q for the electric charge, and μ_S for the strangeness, respectively:

$$f_{\text{Ising}}(T, H) \rightarrow P_{\text{QCD}}(T, \mu_B, \mu_Q, \mu_S, m_q). \quad (18)$$

The one-dimensional temperature space T is thus generalized to a four-dimensional space T, μ_B, μ_Q, μ_S ; variations of the chemical potentials do not affect the intrinsic symmetry of the system. The light quark mass m_q plays, as mentioned, the role of the external field: for $m_q \neq 0$, the chiral symmetry of the Lagrangian is broken explicitly. To illustrate the effect of additional chemical potentials, we consider the baryon number case, simplifying

the notation, $\mu_B = \mu$. The critical point in T thus now becomes a critical line in the $T - \mu$ plane, which renders the relation between variables and critical exponents somewhat more complex, see e.g. [24]. The principle remains the same, however: to find experimental evidence of criticality, we have to look for non-monotonic behavior of response functions measured in heavy ion collisions, to be compared to such behavior obtained in lattice studies. The finite interaction volume in actual collisions, together with time evolution effects, will limit the maximum size of correlations and thus mask a possible divergence. Since the higher derivatives depend on higher powers of ξ , they could provide a more sensitive tool.

The first task is thus to determine in lattice QCD some evidence for critical behavior in the hadronic state, behavior deviating from that of an ideal resonance gas. Here it has to be noted that the partition function in QCD depends on *squared* electric charges and baryochemical potential, since it is left invariant under a change of sign of these quantities. As a result, the non-monotonic behavior shown for the Ising model is shifted to higher order cumulants: the third order spin behavior is expected for the sixth order in QCD, and so on. So far, derivatives up to the second order were seen to agree with the non-critical resonance gas, see Fig. 5(a). First evidence for deviations has been found quite recently [25], studying the sixth order cumulant of the electric charge (χ_6^Q); the result is illustrated schematically in Fig. 8. We see that at the critical point, i.e., at the freeze-out value of the resonance gas, the sixth order cumulant vanishes for QCD, in contrast to the continued monotonic increase expected from the hadronic resonance gas. Such differences are expected to continue for higher orders: the eighth cumulant should become negative in critical QCD, large and positive for the resonance gas. The onset of critical behavior, difficult if not impossible to detect in lower order cumulants, should thus become more and more evident with increasing order.

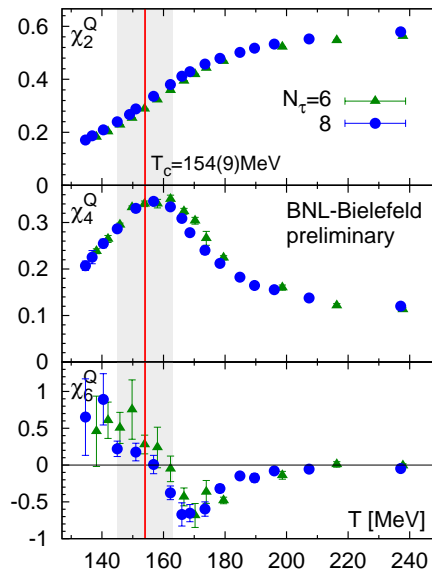


Figure 8: Schematic behavior of the fourth (χ_4^Q) and sixth (χ_6^Q) order cumulants of the electric charge in the critical region, for resonance gas (solid line) vs. lattice QCD calculations (dashed line) [25].

We should here emphasize that the forms shown in Fig. 8 are obtained in physical finite temperature lattice studies, i.e., for 2+1 quark flavors of physical masses, and they give the behavior of the full cumulants, not just a singular part. They are therefore *bona fide* predictions: if these quantities become measurable in heavy ion collisions and there do not show the predicted form, the produced systems are not governed by equilibrium QCD thermodynamics. There can, of course, be various reasons for why this might be the case, up to Feynman’s broken watch, but the result as such would be an observation decisive for our understanding of high energy nuclear collisions.

The search for the critical endpoint will require a similar program, here focused on the baryon density, to be varied by varying the collision energy. The data obtained will again be analysed in terms of the ideal resonance gas, even though we now expect some non-resonant baryon-baryon interactions. And any onset of criticality should produce deviations from monotonic behavior under variations of the collision energy.

Predictions from lattice QCD here are not as readily obtained, since the conventional simulation scheme breaks down for finite μ . Several extensions have been proposed to calculate at least up to some small but finite values. A power series expansion in the baryochemical potential, retaining terms up to second order, gives for cumulant governing baryon number fluctuations the form

$$\chi_B^{(2)}(t, \mu) \sim P^{(2)}(t, \mu = 0) + \mu^2 P^{(3)}(t, \mu = 0), \quad (19)$$

with $t = (T - T_c)/T_c$. The first term is essentially the energy density, the second contains the specific heat. In the case of Z_2 critical behavior, the latter diverges at $t = 0$, and so lattice studies find the pattern shown in Fig. 9, indicating an onset of non-monotonic variation around the critical temperature. The use of the Taylor expansion in μ does not allow this scheme for a determination of the critical point.

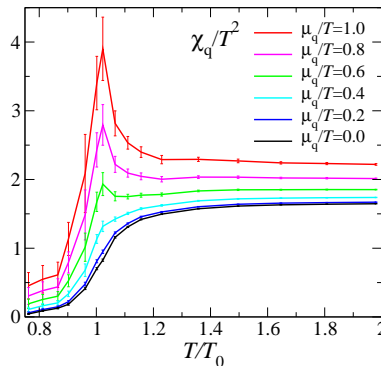


Figure 9: Baryon number susceptibility in two-flavor QCD [26].

The remnant critical behavior of QCD thermodynamics thus is encoded in the higher cumulants of conserved quantum number distributions. Theoretically, these have been and are being studied in considerable detail, for baryon number, electric charge and strangeness. To what extent these are measurable in heavy ion collisions is another issue, beyond the scope of this report. The high statistics experiments at the LHC and the extended beam scan efforts at RHIC give rise to hope for precise enough data, e.g. of charge and baryon number distributions, to allow such studies.

4 The QGP Temperature: Quarkonium Suppression

The ultimate task for nuclear collision studies is evidently to probe if the produced medium in its early pre-hadronic stage is indeed the quark-gluon plasma of QCD. This requires probes present at the pre-confinement stage, and three such probes have been proposed and discussed. Electromagnetic radiation formed in quark interactions can escape from the medium unaffected and thus deliver information about the medium at the time of its formation. Such radiation will, however, also be produced in the hadronic state, and an identification of its origin is difficult. Hard jets are formed at a “hard” early time and must pass through the subsequent pre-hadronic (and hadronic) medium to reach detectors. The energy loss of these jets will reflect the medium being passed, although there are so far no quantitative QCD predictions for this. Heavy charm and bottom quark-antiquark pairs will also be formed at an early time of a scale set by the heavy quark mass. Their fate – open charm/bottom or quarkonium – will reflect the temperature of the medium, indicating if it is too hot for binding or not [27]. Here extensive studies have been carried out over the years, and these will be my final topic.

Because of the heavy mass of charm and bottom quarks, quarkonium spectra can in good approximation be calculated in non-relativistic potential theory; this reproduces the observed (spin-averaged) masses of the ground states as well as of the different excited states to better than a few percent [28]. The resulting binding energies are quite large and the binding radii small, with 600 MeV and 0.2 fm for the charmonium ground state J/ψ , 1.2 GeV and 0.1 fm for the bottomonium ground state Υ . Hence one expects that even in a deconfined medium just above the transition temperature (where the screening radius is around 1 fm), they can still survive as bound states. Only a considerably hotter QGP will eventually prevent binding, both through color screening and through collision dissociation. Raising the temperature of the initial medium through an increase of the collision energy will thus give rise to a step-wise suppression of quarkonia. First the more weakly bound, larger excited states (1P, 2S, ...) will no longer be present, until eventually even J/ψ and Υ must become suppressed.

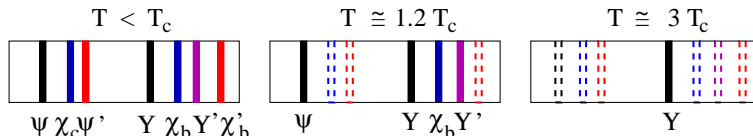


Figure 10: Quarkonium spectral lines as QGP thermometer

To give an indication of the process, we consider the potential theory approach, using the charm system for illustration. The Schrödinger equation

$$\left\{ 2m_c - \frac{1}{m_c} \nabla^2 + V(r) \right\} \Phi_i(r) = M_i \Phi_i(r), \quad (20)$$

with the “Cornell” form for the confining potential [29],

$$V(r) = \sigma r - \frac{\alpha}{r}, \quad (21)$$

in terms of charm quark mass m_c , string tension $\sigma \simeq 0.2 \text{ GeV}^2$ and gauge coupling $\alpha \simeq \pi/12$, then determines the masses M_i and the radii r_i of the different charmonium

states in vacuum. In a hot QGP, the potential is replaced by the color-screened form

$$V(r, T) \sim \sigma r \left\{ \frac{1 - e^{-\mu r}}{\mu r} \right\} - \frac{\alpha}{r} e^{-\mu r}, \quad (22)$$

where $\mu(T)$ specifies the screening mass of the medium and hence $r_c(T) = 1/\mu(T)$ the screening radius. When this falls below the binding radius of a given charmonium state, c and \bar{c} no longer “see” each other and a binding for that state is not possible. Approximating $\mu(T)$ by the form obtained in heavy quark lattice studies leads to suppression thresholds

$$T_{J/\psi} \simeq 1.3 T_c, \quad T_\chi \ \& \ T_{\psi'} \simeq 1.1 T_c. \quad (23)$$

The thresholds for the bottomonium states are shifted to correspondingly higher temperatures.

Such a potential theory treatment is, of course, quite phenomenological. Many attempts have replaced the model input potential (22) by a form obtained directly from heavy quark lattice studies. This still retains ambiguities, however, and it does not include the effect of collision dissociation, which results in an imaginary part of the potential. The *ab initio* approach is to calculate the in-medium quarkonium spectrum directly in finite temperature lattice QCD, and since several years that endeavor is under way by various groups [30–36]. In these calculations, the quarkonium correlator $G(\tau, T)$ is determined at temperature T ; it is an integral transform of the desired quarkonium spectrum $\sigma(\omega, T)$,

$$G_i(\tau, T) = \int d\omega \sigma_i(\omega, T) \frac{\cosh[\omega(\tau - (1/2T))]}{\sinh(\omega/2T)}. \quad (24)$$

In principle, the transform just has to be inverted to obtain the spectrum; in practice, the correlator is given only on for a finite number of points in τ , which makes the inversion ambiguous. It is therefore generally carried out by the *Maximum Entropy Method*, a scheme to reconstruct something based on fragmentary information [37]. So also here the last word is not yet said, though with increased computer performance and size, the results are constantly gaining in certainty. Some as yet not final, though perhaps indicative results are shown in the following table.

state	$J/\psi(1S)$	$\chi_c(1P)$	$\psi(2S)$	$\Upsilon(1S)$	$\chi_b(1P)$	$\Upsilon(2S)$	$\chi_b(2P)$	$\Upsilon(3S)$
T_d/T_c	1.5	1.1	1.1	> 4.0	1.8	1.60	1.2	1.1

For bottomonium, a recent temperature scan [38] based on lattice studies in non-relativistic QCD provides some more details of the suppression pattern for the higher excited states. The results are shown in Fig. 11.

Once the final answers are given, we can specify up to what temperature the survival of a given quarkonium state in a hot QGP is possible, and moreover give the ratios of the different survival thresholds.

To discuss the effect of this on quarkonium production, we first recall underlying dynamics, again using the J/ψ for illustration. The production process in elementary hadronic collisions (taking pp as example) begins with the formation of a $c\bar{c}$ pair; this pair can

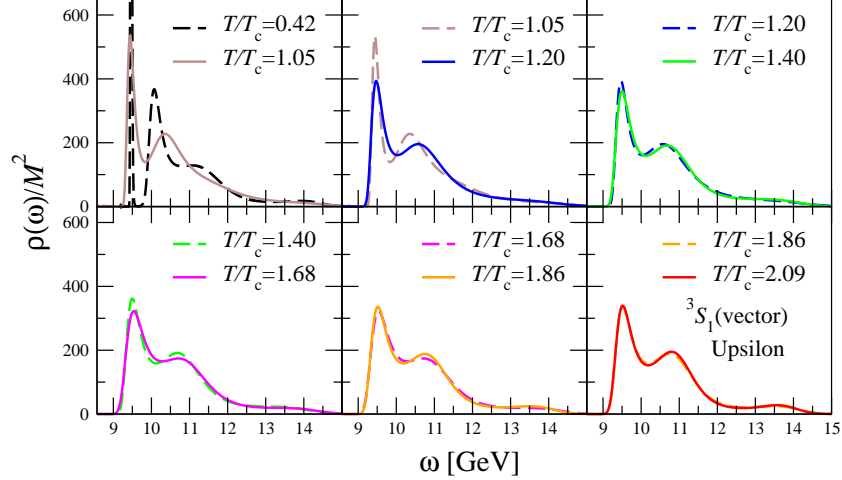


Figure 11: Suppression patterns for bottomonia in NRQCD [38]

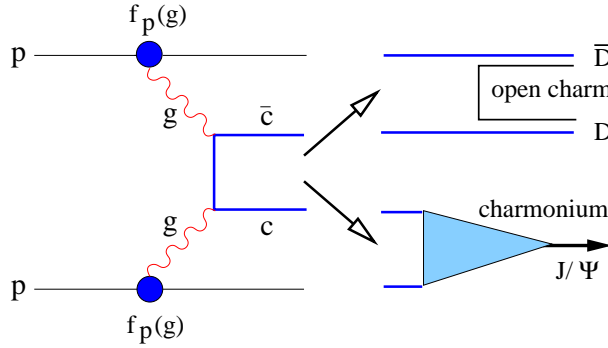


Figure 12: Schematic view of J/ψ production in pp collisions

then either lead to open charm production (about 90 %) or subsequently bind to form a charmonium state (about 10 % for all charmonia). A schematic illustration (Fig. 12) shows the dominant high energy reaction through gluon fusion.

The initial $c\bar{c}$ production can be calculated in terms of the parton distribution functions f_p of the relevant hadrons and the perturbative partonic cross section. The full description of charmonium binding has so far resisted various theoretical attempts; on the other hand, the process is in good approximation independent of the incident hadronic collision energy [39, 40]. This is a consequence of the fact that the heavy quark propagator in the reaction $gg \rightarrow c\bar{c}$ strongly dampens the mass variation of the $c\bar{c}$ pair with incident energy. Thus the fractions of the produced $c\bar{c}$ system into hidden vs. open charm as well as those for the different charmonium states are approximately constant; once determined at one energy, they remain the same also for different collision energies. As a result, the phenomenological color evaporation model [41–44] provides a good description of charmonium production through the form

$$\sigma_{hh \rightarrow J/\psi}(s) = g_{c\bar{c} \rightarrow J/\psi} \sigma_{hh \rightarrow c\bar{c}}(s), \quad (25)$$

and correspondingly for the other charmonium states. Here the constant $g_{c\bar{c} \rightarrow J/\psi}$ specifies what fraction of the total $c\bar{c}$ production cross section goes into J/ψ production; in pp collisions it is typically about 2 %. The set of the different constants $g_{c\bar{c} \rightarrow i}$ for the different

charmonium states i thus effectively characterizes charmonium production in the absence of a medium.

A further important aspect of quarkonium production in elementary collisions is that the observed (1S) ground states J/ψ and Υ are in both cases partially produced through feed-down from higher excited states [45–48]. Of the observed J/ψ rates, only some 60 % is a directly produced $J/\psi(1S)$ state; about 30 % comes from $\chi_c(1P)$ and 10 % from $\psi'(2S)$ decay. Because of the narrow width of the excited states, their decay occurs well outside any interaction region.

The features we have here summarized for charm and charmonium production are readily extended to that of bottom and bottomonium. To simplify the discussion, we shall continue referring to the charmonium case, keeping in mind that all arguments apply as well to bottomonia. Given the patterns observed in elementary collisions, we want to see how they are modified in the presence of a medium, as provided by nuclear collisions. From the point of view of production dynamics, one way such modifications can arise is as *initial state effects*, which take place before the $c\bar{c}$ pair is produced. The main possibilities considered so far are nuclear modifications of the parton distribution functions (shadowing or antishadowing) and a possible energy loss of the partons passing through the nuclear medium to produce the $c\bar{c}$. Once produced, the pair can encounter *final state effects*, either in the form of a phase space shift already of the $c\bar{c}$, e.g., through an energy loss of the unbound charm quarks, or through effects on the nascent or fully formed charmonium state. Such effects may arise from the passage through the cold nuclear medium, or because of the presence of the medium newly produced in the nuclear collision. The latter is evidently what we have in mind when we want to use quarkonia to study quark-gluon plasma production.

Next we turn to quarkonium binding in a hot medium. Color screening in a quark-gluon plasma will decrease the binding force, both in strength and in its spatial range, and this should for sufficiently energetic nucleus-nucleus collisions suppress quarkonium formation. In addition, there will be collision break-up. Since the larger and less tightly bound states will be suppressed at lower temperature or energy density than the ground states, the result will be *sequential suppression* [49, 50]. We illustrate this for the J/ψ . After an initial threshold suppressing the ψ' and hence removing its feed-down component for J/ψ production, there will be a second threshold for χ_c suppression and then finally a third, at which the direct $J/\psi(1s)$ is dissociated. The resulting pattern is illustrated in Fig. 13. We have here introduced something denoted as J/ψ survival probability: the chance of a J/ψ to persist as a bound state in a deconfined medium. A similar sequential suppression pattern will arise for the step-wise removal for the higher state contributions to Υ production; both quarkonium patterns are shown in Fig. 13.

We had already introduced the concept of quarkonium survival; that has to be specified more explicitly. Since we are interested in using quarkonium production as a tool to study the medium produced in nuclear collisions, our primary concern is not if such collisions produce more or fewer $c\bar{c}$ pairs than proton-proton collisions, but rather if the presence of the medium modifies the fraction of produced $c\bar{c}$ pairs going into charmonium formation. In other words, the crucial quantity is the amount of charmonium production relative to that of open charm [51, 52]. To illustrate: in pp collisions, about 2 % of the total $c\bar{c}$ production goes into J/ψ 's. If in high energy nuclear collisions the total $c\bar{c}$ production rate were reduced by a factor two, but we still have 2 % of these going into J/ψ 's, then evidently

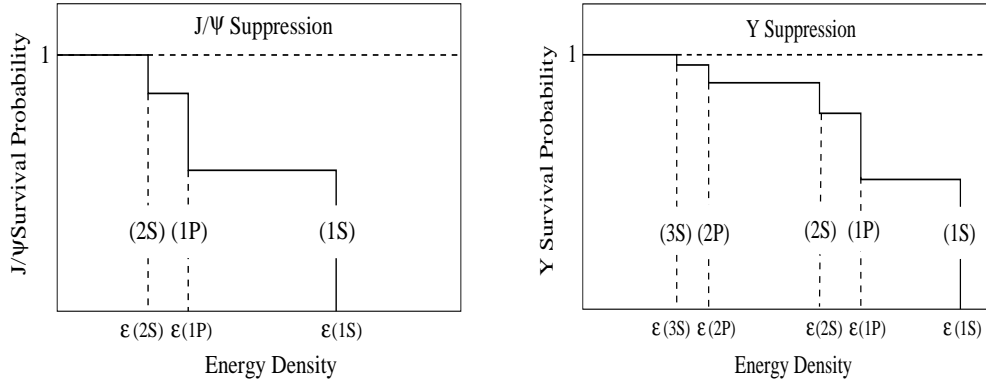


Figure 13: Sequential quarkonium suppression

AA collisions do not modify J/ψ binding. Hence the relevant observable is the fraction of charmonia to open charm, or more generally, that of quarkonia to the relevant open heavy flavor production [51–53]. In this quantity, if measured over the entire phase space, the effects of possible initial state nuclear modifications – shadowing/antishadowing, parton energy loss – cancel out, so that whatever changes it shows relative to the pp pattern is due to final state effects.

Possible alternative variables to consider are the production ratios of the different quarkonium states; this has very recently become of particular interest for bottomonium studies. Since $\Upsilon(1S)$, $\Upsilon(2S)$ and $\Upsilon(3S)$ lie quite close to each other in mass, in the ratio of their rates again initial state effects are expected cancel out.

Let me close by commenting briefly on the experimental status. J/ψ suppression in nuclear collisions, when compared to pp collisions, was observed from the very beginning. Those data have, however, remained inconclusive for some twenty-five years, essentially because the crucial observables were not available. Lack of open charm data was compensated by comparison to pp data, and this brought in uncontrollable uncertainties due to initial state effects. These effects were measured in pA interactions, modelled and then used to construct AA predictions, which necessarily remained model-dependent. Since a few years, open charm data have become available, so that it is only a matter of time now before the crucial variables can be experimentally determined.

For charmonia, measuring open to hidden flavor is moreover of interest for yet another reason. The abundance of $c\bar{c}$ pair production at LHC energy has led to the suggestion that at hadronisation a c from one collision may statistically combine with a \bar{c} from another, thus providing a new secondary charmonium production mechanism. Even with all primary J/ψ suppressed, such statistical combination could lead to an abundant new production at hadronisation [54–57]. Again here the prediction is a reshuffling of the $c\bar{c}$ pairs between hidden and open charm channels, so that only a measurement hidden/open can provide an unambiguous answer. If such a mechanism is indeed effective, the sequential pattern we had discussed is no longer present; instead, the ratios are those of the hadrosynthesis of the charm sector. Evidently, this would constitute strong evidence for a thermal quark-gluon plasma.

The role of the QGP thermometer would in that case be played by bottomonium production. We therefore close this section with some recent data on this, data which provides

perhaps the first clear evidence for sequential suppression [58]. In Fig. 14 the bottomonium spectrum in pp collisions is compared to that in $Pb-Pb$ collisions, both measured at the LHC for $\sqrt{s} = 2.75$ TeV. In nuclear collisions, the higher excited states $\Upsilon(2S)$ and $\Upsilon(3S)$ are strongly suppressed relative to the ground state $\Upsilon(1S)$. The production rate for this, however, is also found to be reduced there, essentially by the contributions it received in pp interactions through feed-down from excited states. This becomes more evident in the right panel of Fig. 14(c), where the scaled background curves are matched.

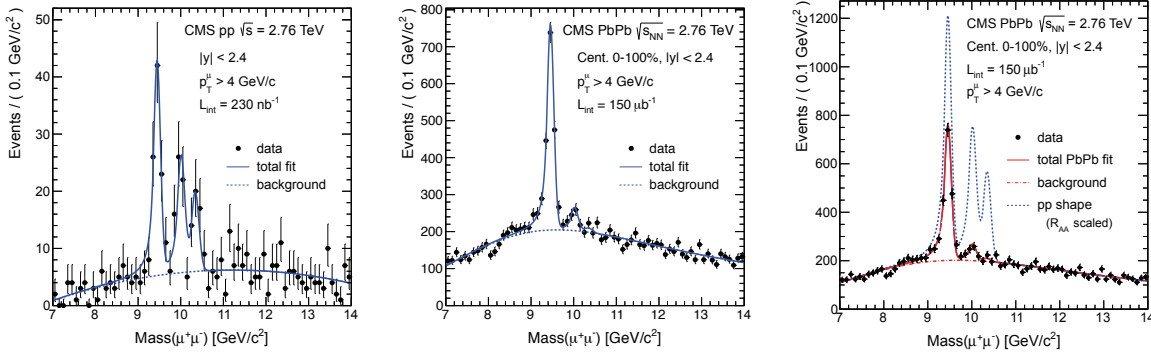


Figure 14: Bottomonium production in pp (left) and $Pb-Pb$ (right) collisions, as measured by the CMS collaboration at CERN-LHC [58]

5 Conclusions

Our aim was to focus on how in high energy nuclear collisions one can test predictions from equilibrium statistical QCD. We showed in particular that

- nuclear collisions at low baryon density produce a hadronic medium in thermal equilibrium at the confinement temperature found in lattice QCD;
- the critical behavior at the hadronization transition is encoded in fluctuations calculated in QCD, and these are in principle measurable for baryon number, charge and strangeness;
- the suppression thresholds of quarkonium states specify the temperature of the QGP; they are calculable in lattice QCD and measurable for charmonia (caveat: regeneration through statistical combination) and bottomonia.

References

- [1] T. Renk, *Theory of Heavy-Ion Collisions*, 24th International Symposium on Lepton-Photon Interactions at High Energies, DESY, Hamburg, Germany, August 17-22, 2009; Conf. Proc. C0908171 (2009) 93; arXiv:1001.2452.
- [2] J.-Y. Ollitrault, *Heavy Ion Theory*, 25th International Symposium on Lepton-Photon Interactions at High Energies, Tata Institute of Fundamental Research, Mumbai, India, August 22-27, 2011.

- [3] R. Pisarski and F. Wilczek, *Phys. Rev. D* **29** (1984) 338.
- [4] O. Kaczmarek et al., *Phys. Rev. D* **83**, 014504 (2011) [arXiv:1011.3130].
- [5] A. M. Halasz et al., *Phys. Rev. D* **58**, 096007 (1998) [hep-ph/9804290].
- [6] M. A. Stephanov, K. Rajagopal and E. V. Shuryak, *Phys. Rev. Lett.* **81**, 4816 (1998) [hep-ph/9806219].
- [7] Y. Hatta and T. Ikeda, *Phys. Rev. D* **67** (2003) 014028.
- [8] A. Bazazov et al. (Hot QCD), *Phys. Rev. D* **85** (2012) 065503.
- [9] E. Beth and G. E. Uhlenbeck, *Physica* **4** (1937) 915.
- [10] R. Dashen, S.-K. Ma and H. J. Bernstein, *Phys. Rev.* **187** (1969) 345.
- [11] J. Cleymans et al., *Phys. Lett. B* **242** (1990) 111.
- [12] J. Cleymans and H. Satz, *Z. Phys. C* **57** (1993) 135.
- [13] K. Redlich et al., *Nucl. Phys. A* **566** (1994) 391.
- [14] P. Braun-Munzinger et al., *Phys. Lett. B* **344** (1995) 43.
- [15] F. Becattini, M. Gazdzicki and J. Sollfrank, *Eur. Phys. J.* **5** (1998) 143.
- [16] F. Becattini et al., *Phys. Rev. C* **64** (2001) 024901.
- [17] F. Becattini et al., *Phys. Rev. C* **85** (2012) 044921.
- [18] J. Letessier, J. Rafelski and A. Tounsi, *Phys. Rev. C* **64** (1994) 406.
- [19] P. Castorina, D. Kharzeev and H. Satz, *Eur. Phys. J.* **52** (2007) 187.
- [20] F. Becattini et al., *Eur. Phys. J.* **56** (2008) 493.
- [21] P. Castorina and H. Satz, work in progress
- [22] M. M. Aggarwal et al. (STAR Collaboration), *Phys. Rev. Lett.* **105** (2010) 22302
- [23] F. Karsch and K. Redlich, *Phys. Lett. B* **695** (2011) 136.
- [24] O. Kaczmarek et al., *Phys. Rev. D* **83**, 014504 (2011) [arXiv:1011.3130 [hep-lat]].
- [25] Christian Schmidt, *Nucl. Phys. A* **904-905** **2013**, 865c (2013) [arXiv:1212.4278 [hep-lat]].
- [26] S. Ejiri et al., *Phys. Rev. D* **80** (2009) 094505.
- [27] T. Matsui and H. Satz, *Phys. Lett. B* **178** (1986) 416.
- [28] S. Jacobs, M. G. Olsson and C. Suchyta, *Phys. Rev.* **33** (1986) 3338.
- [29] E. Eichten et al., *Phys. Rev. D* **17** (1978) 3090; *Phys. Rev. D* **21** (1980) 203.

- [30] T. Umeda et al., *Int. J. Mod. Phys. A*16 (2001) 2215.
- [31] M. Asakawa and T. Hatsuda, *Phys. Rev. Lett.* 92 (2004).
- [32] S. Datta et al., *Phys. Rev. D* 69 (2004) 094507
- [33] H. Iida et al., *PoS LAT2005* (2006) 184.
- [34] A. Jacovac et al., *Phys. Rev. D* 75 (2007) 014506.
- [35] R. Morrin et al., *PoS LAT2005* (2006) 176;
G. Aarts et al., *Nucl. Phys. A* 785 (2007) 198.
- [36] H. T. Ding et al., *Phys. Rev. D* **86**, 014509 (2012) [arXiv:1204.4945 [hep-lat]].
- [37] Y. Nakahara, M. Asakawa and T. Hatsuda, *Phys. Rev. D* 60 (1999) 091503.
- [38] G. Aarts et al., *JHEP* **1111**, 103 (2011) [arXiv:1109.4496 [hep-lat]].
- [39] R. Gavai et al., *Int. J. Mod. Phys. A*10 (1995) 3043.
- [40] R. Vogt, *Quarkonium Baseline Predictions*, in *Hard Probes in Heavy-Ion Collisions at the LHC*, M. Mangano, H. Satz and U. Wiedemann (Eds.), CERN Yellow Report 2004-009.
- [41] M. B. Einhorn and S. D. Ellis, *Phys. Rev. D*12 (1975) 2007.
- [42] H. Fritzsch, *Phys. Lett.* 67B (1977) 217.
- [43] M. Glück, J. F. Owens and E. Reya, *Phys. Rev. D*17 (1978) 2324.
- [44] J. Babcock, D. Sivers and S. Wolfram, *Phys. Rev. D*18 (1978) 162.
- [45] L. Antoniazzi et al. (E705 Collaboration), *Phys. Rev. Lett.* 70 (1983) 383.
- [46] P. Faccioli et al., *JHEP* 0810:004 (2008).
- [47] A. Adare et al. (PHENIX Collaboration), arXiv:1105.1966[hep-ex].
- [48] N. Brambilla et al. (QWG), *Heavy Quarkonium Physics*, CERN -2005-005.
- [49] F. Karsch and H. Satz, *Z. Phys. C* 51 (1991) 209.
- [50] D. Kharzeev, F. Karsch and H. Satz, *Phys. Lett. B* 637 (2006) 75.
- [51] K. Sridhar and H. Satz, *Phys. Rev. D*50 (1994) 3557.
- [52] H. Satz, *Adv. High Energy Phys.* 2013 (2013) 242918 [arXiv:1303.3493 [hep-ph]].
- [53] A. Andronic, P. Braun-Munzinger and K. Redlich, *Nucl. Phys. A*789 (2007) 334.
- [54] P. Braun-Munzinger and J. Stachel, *Nucl. Phys. A*690 (2001) 119.
- [55] R. L. Thews et al., *Phys. Rev. C* 63 (2001) 054905.

- [56] L. Grandchamp and R. Rapp, Nucl. Phys. A 709 (2002) 415.
- [57] M. Mangano and R. L. Thews, Phys. Rev. C 73 (2006) 014904.
- [58] S. Chatryan et al. [CMS Collaboration], Phys. Rev. Lett. 109 (2012) 222301.